Realizing complex carbonate facies, diagenetic and fracture properties with standard reservoir modelling software

MICHAEL C. PÖPPELREITER[1], MARIA A. BALZARINI[2], BIRGER HANSEN[3] & RONALD NELSON[4]

[1]*Qatar Shell Research and Technology Centre, PO 3747, Doha, Qatar (e-mail: m.poppelreiter@shell.com)*

[2]*Shell International E&P, 200N Dairy Ashford, Houston, Texas, 77049, USA*

[3]*Eriksfiord AS, Chausee de Fleurus 6040, Jumet, Belgium*

[4]*Broken N Consulting Inc., 445 Wrangler Road, Simonton, Texas, 77476-1017 USA*

Abstract: Geocellular modelling of diagenetically altered carbonates is challenging as geometries and pore systems often appear irregular. It has long been recognised, however, that tectonic evolution forms a framework that can influence patterns of carbonate facies, diagenesis and fracturing, the combination of which determines reservoir geometries and properties. Unravelling these processes can reveal trends that were not evident from well data alone. Such trends are useful in building geocellular models that extrapolate reservoir properties along them and can be used for economic screening of undrilled areas. This paper shows how standard reservoir modelling software can be used to model complex geology. In particular, it is shown how a carbonate reservoir model was constructed based on concepts of facies, burial diagenesis, hydrocarbon charge and fracturing. Workflows are discussed that were employed to distribute reservoir properties related to these processes.

The Maracaibo Basin in north-west Venezuela (Fig. 1) is one of the oldest petroleum provinces in the world. One of the key producing intervals is the Cogollo Group (Fig. 1), a deeply buried (5000–6000 m) limestone reservoir. This study concerns the Urdaneta West field, which, in contrast to other Cogollo fields in the Maracaibo Basin, is not a fracture-only play. It produces primarily from grain-dominated beds with secondary (leached) porosity as well as fractures. These pore types created a complex reservoir architecture (Fig. 2) that constitutes the main uncertainty for field development. Wells in the Urdaneta West field only produce at economic rates when they encounter sufficient porosity-height, i.e. leached grainy layers. Thus, the prediction of sufficient matrix porosity is of key economic importance. Average porosities and permeabilities are low, $<3\%$ and <0.01 mD, respectively (Fig. 3). However, locally, porosities between 10% and 20% and permeabilities in the tens of a millidarcy are common (Fig. 3). These rock properties are significantly higher than would be expected at present burial depths (Scholle & Halley 1985; oral communication P. Wagner 2002; Ehrenberg & Nadeau 2005). This is attributed to the fact that a significant proportion of the pore volume is secondary (vuggy) in nature, probably due to burial diagenesis. Additionally early hydrocarbon charge of structurally elevated parts of the field might have reduced post-leaching cementation in certain areas and subsequent fracturing might link up 'matrix sweet spots'.

Geological setting

The Cogollo Group, of Aptian to Albian age (Renz 1981), was deposited in the Maracaibo Basin. This basin extended some 50 000 km^2 across portions of north-west Venezuela, Peru, Ecuador and Colombia (Castillo & Mann 2006). It was part of the Lower Cretaceous passive continental margin (Vahrenkamp *et al*. 1993) (Fig. 3). The Cogollo Group in the study area is some 370 m (1200 ft) thick and composed of thin shoal packstones and grainstones (potentially containing matrix porosity) intercalated with thick lagoonal wackestones and mudstones (tight, potentially fractured) (Bartok *et al*. 1981). Global sea-level rise and greenhouse conditions triggered platform growth over a thin veneer of continental clastics or in some areas directly upon basement rocks. Oscillations of relative sea level led to migrations of the carbonate ramp and development of six large-scale depositional sequences (Azpiritxaga 1991).

From: Robinson, A., Griffiths, P., Price, S., Hegre, J. & Muggeridge, A. (eds) *The Future of Geological Modelling in Hydrocarbon Development*. The Geological Society, London, Special Publications, **309**, 39–49.
DOI: 10.1144/SP309.3 0305-8719/08/$15.00

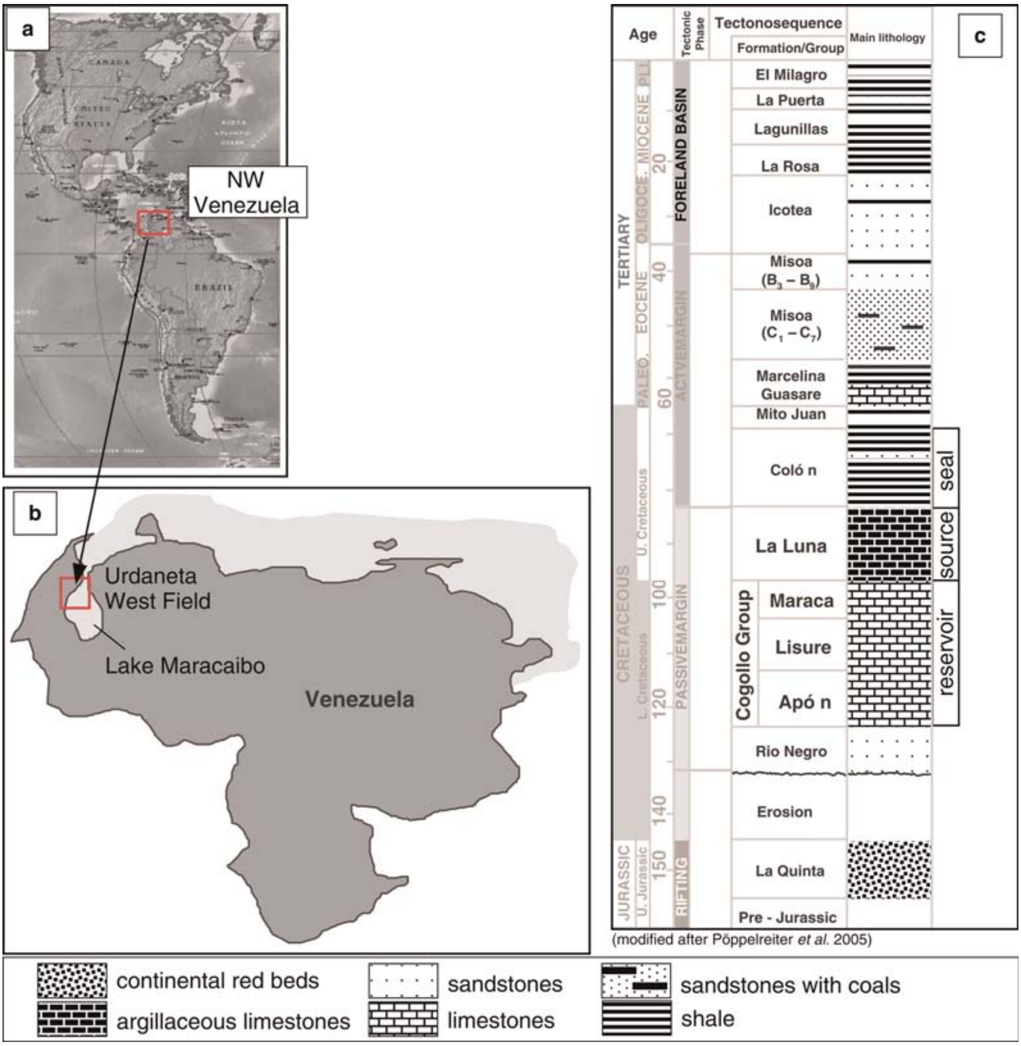

Fig. 1. (**a**) Location of the Urdaneta West field in NW Venezuela. (**b**) Location of the Urdaneta West field at the western margin of Lake Maracaibo. (**c**) Stratigraphy of the Urdaneta field. Indicated are the main stages of basin development in NW Venezuela and the components of the Cogollo Play.

Database

The dataset used in this study includes all available cores and cuttings from the Urdaneta West field. Seismic was re-evaluated, from a reprocessed 3D seismic volume (Fig. 3), with emphasis put on structural features. A detailed and consistent re-evaluation of openhole logs from 56 wells was performed. Furthermore, 17 borehole image logs were re-interpreted focusing on fractures, stress indicators and secondary porosity. This analysis was accompanied by a quick-look study of 14 dip-meter logs as well as rock strength and acoustic measurements from core plugs. Additionally, detailed basin modelling results were integrated and supported by an extensive literature review. Integrated sedimentologic-stratigraphic, petrophysic and dynamic analyses provided the ingredients for the conceptual reservoir model discussed below (Fig. 4).

Facies and thickness

Observations

Gross reservoir thickness at Urdaneta West is well constrained by more than 50 well penetrations.

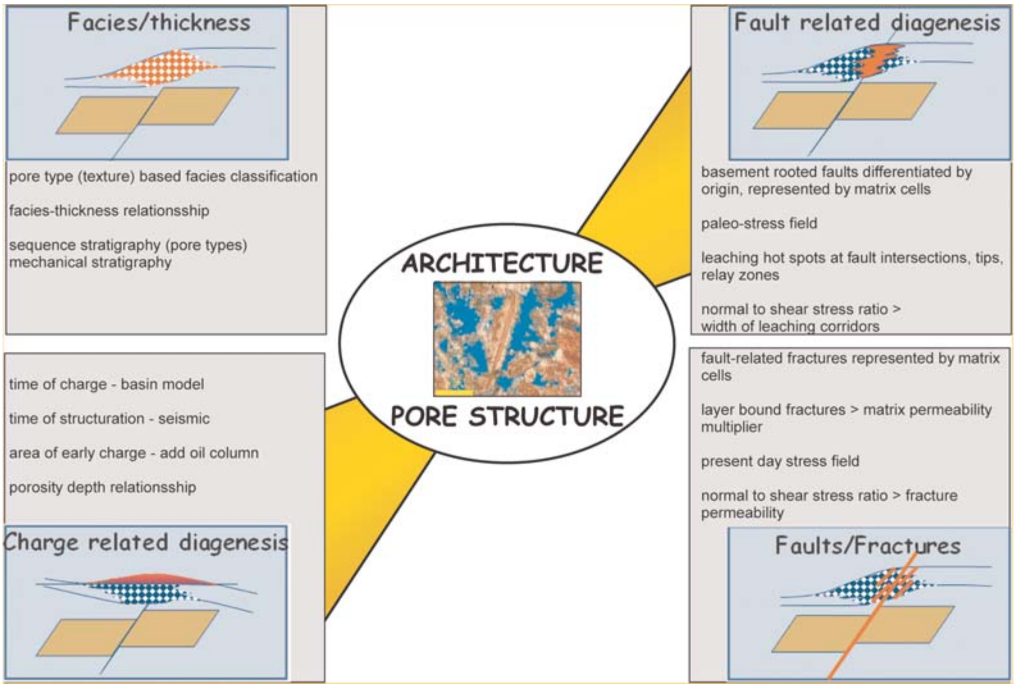

Fig. 2. The interplay of facies, fault/fracture, fault- and charge-related diagenesis are major factors influencing the complex reservoir architecture and pore structure in carbonate reservoirs diagenetically altered during burial.

Facies distribution is well known from cores, cuttings, openhole logs and borehole image logs at the field crest but poorly constrained at the flanks. Petrographic analysis showed that economically significant porosity is present only in grainy facies, i.e. skeletal packstones and grainstones (Fig. 4) that occur in a cyclic fashion. Stacking pattern controls the vertical occurrence of grainy facies. Thick packages with the highest percentage of grainy layers occur mostly at the transgressive base and the regressive top of medium-scale stratigraphic cycles.

Six large-scale stratigraphic cycles were correlated regionally across the carbonate platform for some 300 km using core-calibrated wells. The cross-sections revealed an aggradational facies architecture with thin grainstone sheets extending for tens of kilometres (Fig. 5). Cross-sections support observations of earlier workers that packstones and grainstones preferentially occur on palaeohorst blocks (Bartok *et al.* 1981), suggesting antecedent topography influenced facies distribution (Lomando 1999). Gross reservoir thickness on such palaeohorst blocks is lower compared to palaeograben areas; net reservoir thickness however can be higher.

Thickness maps of large-scale stratigraphic units were constructed (Fig. 5). These maps were superimposed on gravity, magnetic and seismic fault traces. It appears that smaller thickness, particularly in the lower part of the reservoir Apon Formation, corresponds to low gravity and low magnetic susceptibility and seems aligned with NE–SW striking horst blocks (Bartok *et al.* 1981; Lugo 1991). Cores, cutting logs and outcrop data show a subtle trend of more muddy textures with increasing gross thickness away from horst blocks. Decreasing thickness of large-scale stratigraphic units corresponds to horst blocks with slower subsidence and a higher percentage of grainy shoal beds.

Modelling

A layering scheme, based on sequence stratigraphic units, was established that separated layers with specific textures and pore types. The lateral variability within each layer is limited on field scale. A facies model was then built with the two major rock types: grainy, skeletal packstone and grainstone and muddy, tight mudstone and wackestone (Fig. 5). These were distributed stochastically using trend maps. Trends were applied in poorly constrained areas away from current well control. The perceived control of facies by antecedent topography was used as circumstantial evidence to model facies with thickness trends. Thus, the

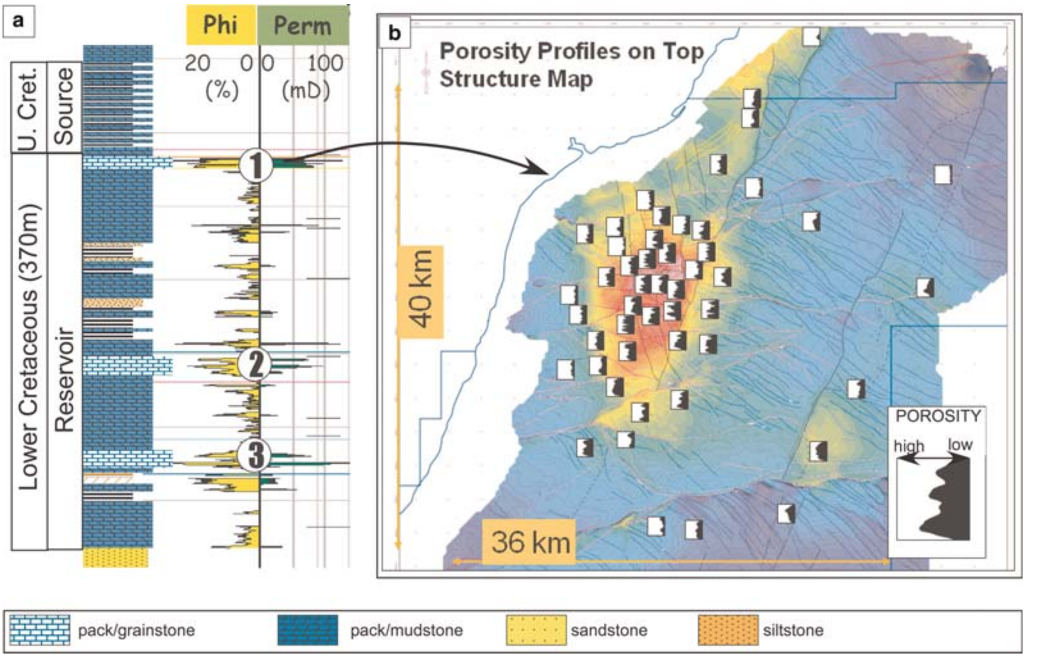

Fig. 3. (**a**) Type section of the Cogollo Group at Urdaneta West. The 370 m thick Cogollo Group is deposited above Lower Cretaceous Rio Negro sandstones. The reservoir is covered by Upper Cretaceous La Luna argillaceous limestones (source rock). The Cogollo limestones are generally tight with three layers with matrix porosity and permeability. (**b**) Porosity profiles of the uppermost porous layer plotted on a top Cogollo structure depth map (red colours indicate high areas whereas dark blue colors show the structurally deepest areas). Note the large amount of seismically visible faults. Different colours of the fault indicate a different origin of these faults.

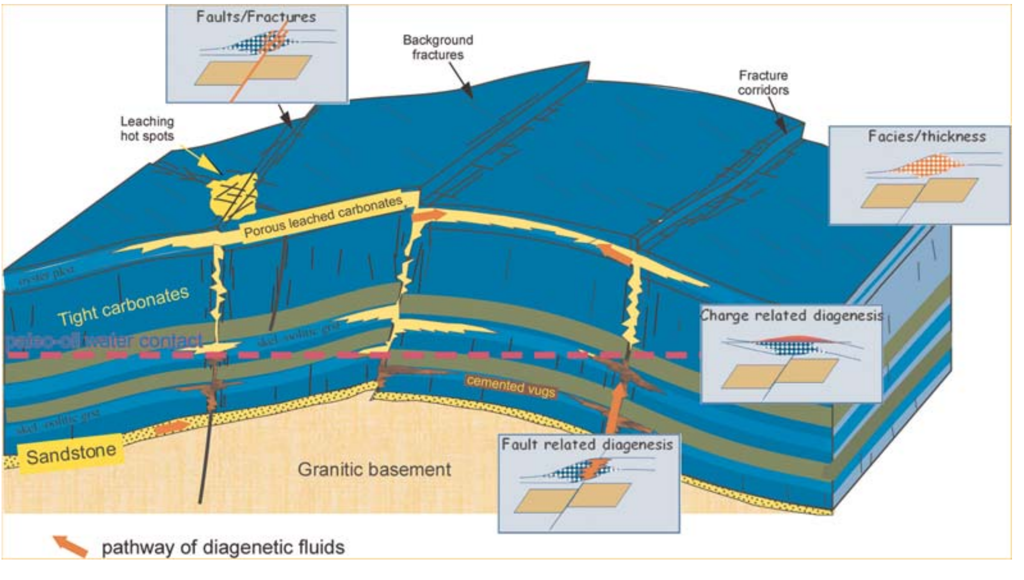

Fig. 4. Conceptual model showing the distribution of vuggy pores and fractures in the Cogollo reservoir. The tectonic evolution plays a major role in the development of porosity.

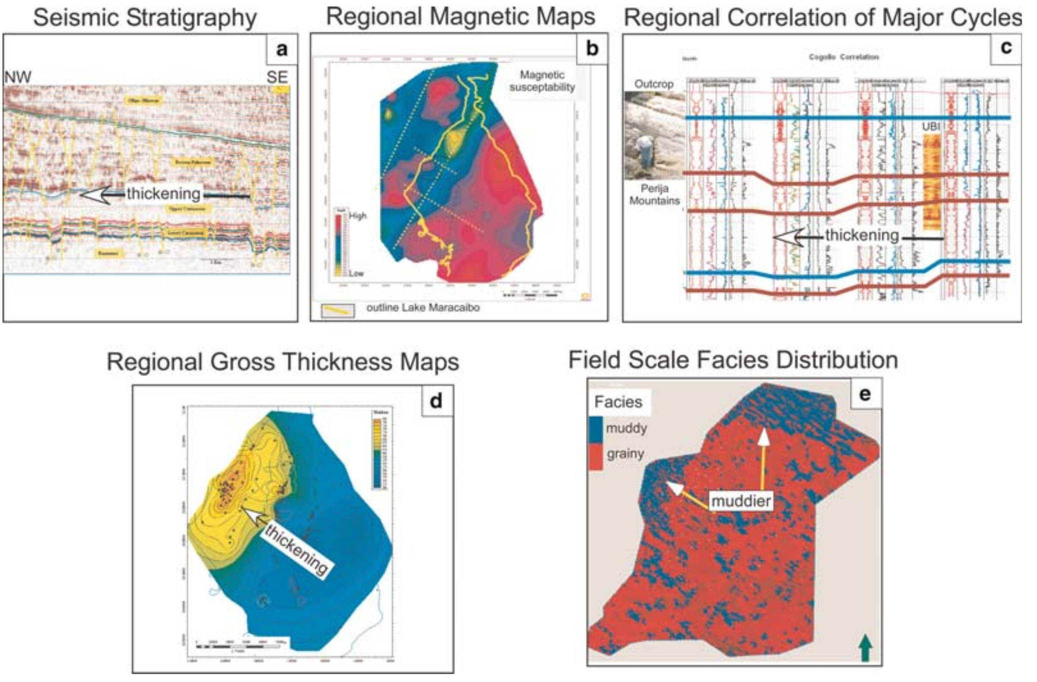

Fig. 5. Workflow to derive a facies model by integrating local and regional information. (**a**) Seismic stratigraphy is used to identify and map thicknesses of large-scale stratigraphic units. (**b**) Gravity and magnetic maps are checked to understand regional orientation and boundaries of major structural units. (**c**) Well-log correlation of intra-reservoir (Cogollo Group) cycles linked with facies analysis can show syn-depositional thickness and facies trends. (**d**) Thickness map of intra-reservoir cycle compared to other property maps might reveal common pattern which can be used as circumstantial evidence for field-scale models. (**e**) The summary of the observations can help to construct more accurate facies trends at field scale.

percentage of grainy textures was gradually decreased with increasing gross thickness (Fig. 5).

Fault-related diagenesis

Observations

Most porosity was secondary in nature, either biomouldic or vuggy (solution enlarged) that occurred almost exclusively in skeletal packstones and grainstones. Interestingly, vuggy pores were associated with ‘exotic cement phases’ such as baroque dolomite, authigenic kaolinite, and chalcedony (Vahrenkamp *et al*. 1993). These show a geochemical signature, i.e. salinity, temperature, isotopes, incompatible with the original depositional system. Diagenetic phases, mentioned above, are similar in secondary pores and fractures. This suggests a late burial origin of these pores (Esteban & Taberner 2003). Moreover, elevated secondary porosity in existing wells seems to occur mostly in the vicinity of seismic-scale basement-rooted faults.

Secondary porosity along basement-rooted faults (Knipe 1993) is well known from various reservoirs (Hurley & Budros 1990; Wilde & Muhling 2000; Boreen & Colquhoun 2003; Tinker *et al.* 2004; Davies & Smith 2006). The geometries of fault-related leaching zones are also documented from outcrop analogue studies (Wilson 1990; Lopez-Horgue *et al*. 2005). The examples mentioned are possible analogues for the diagenetic alterations at Urdaneta West.

Accordingly, corrosive fluids migrated through a sandstone aquifer at the base of the Cogollo Group, the Rio Negro Formation (Fig. 2). The most effective vertical pathways for corrosive fluids are expected to be critically stressed strike-slip faults, fault tips and relay zones (Hickman *et al*. 2003; see also Fig. 5d). The pre-existing texture-controlled porosity and permeability network influenced the lateral distance fluids migrated into the formation. Porosity and permeability of diagenetic zones varies laterally from leached/fractured rocks along fault zones with permeabilities of over 100 mD, to lightly leached matrix rocks with maximum permeabilities of a few millidarcies located a few kilometres onto the platform. Width of leached zones can vary from only a few metres in tight rocks up to several kilometres in more permeable rocks. Timing of leaching with respect to compaction is critical in creating sufficient secondary porosity. Vertically, the strongest leaching is observed beneath low permeability shales and argillaceous carbonates, which might have hindered ascent of corrosive fluids and forced them laterally into slightly better permeable layers.

Modelling

The structural history from the Cretaceous to present day was re-evaluated from a reprocessed 3D seismic volume to characterize faults as possible pathways for diagenetic fluids. Basement-rooted faults were separated from shallow overburden faults. All Miocene and shallow overburden faults were ignored in terms of the leaching process.

Basement-rooted faults were subdivided into Upper Carboniferous (ENE striking), Jurassic (NNE striking) and Eocene (NNW striking) faults, based on seismic stratigraphy and attribute analysis (Galarraga *et al.* 2005). Leaching corridors were only modelled along basement-rooted faults, which were present during the Eocene, the inferred time of leaching (Fig. 6). The lateral extent of leached rock, i.e. areas of elevated porosity, was modelled as a function of texture, fault length, rugosity, structural history and stress state at the inferred time of leaching. The stress state of all basement-rooted fault zones (Fig. 6) was approximated with a geomechanical workflow following

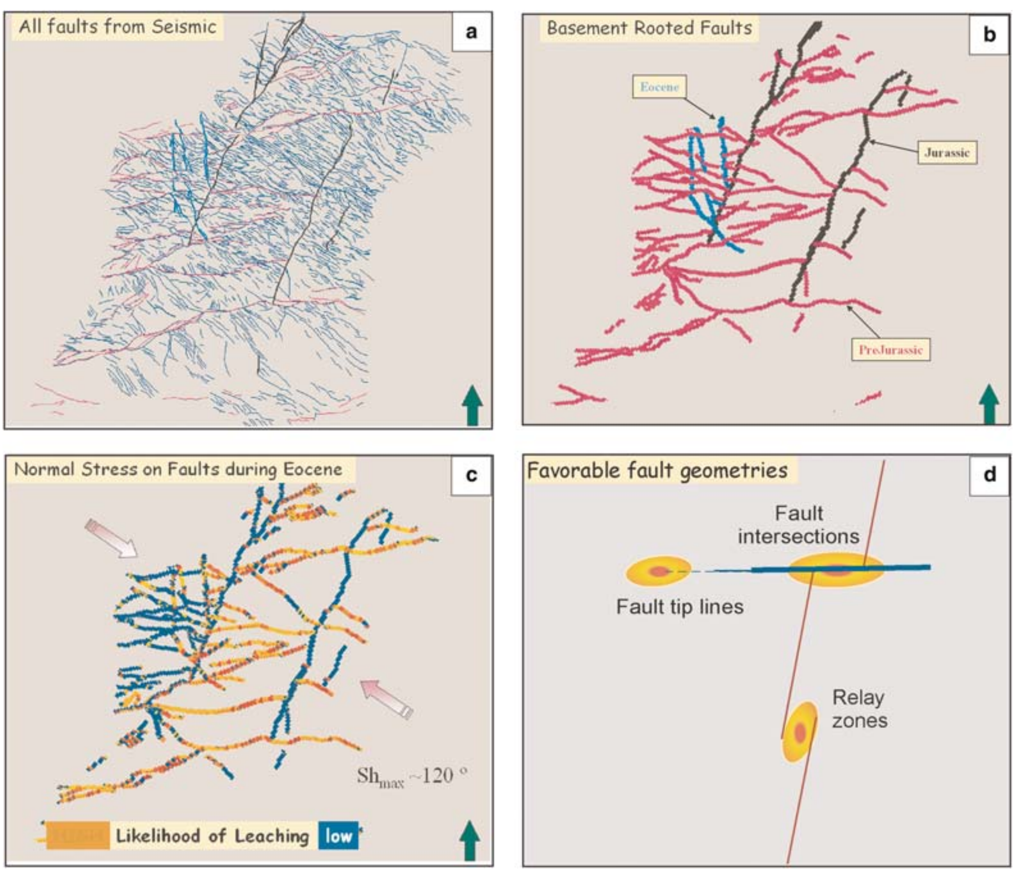

Fig. 6. Workflow to identify likely leached fault compartments that are suspected to have aureoles with elevated porosities along them. (**a**) All seismic scale faults interpreted at Urdaneta West. (**b**) Only basement-rooted faults, which are differentiated according to their origin into Pre-Jurassic (Upper Carboniferous) (pink), Jurassic (black) and Eocene (light blue) faults. (**c**) Faults are differentiated by stress values (an output parameter of the geomechanical algorithm), which is scaled to relatively high or low likelihood of leaching. (**d**) Fault intersections, interaction areas and fault top lines, along the basement-rooted faults (compare Fig. 6b) are additional locations of possible leaching.

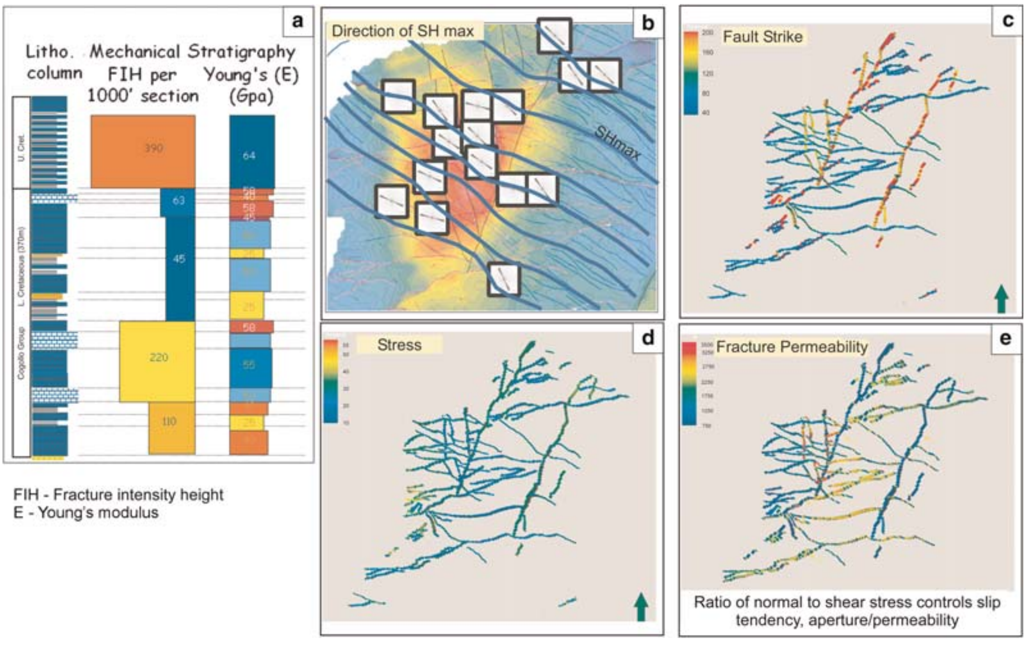

Fig. 7. The sequence of figures shows input parameters/results of the geomechanical model used to assess the leaching potential of fault segments. (**a**) Mechanical stratigraphy built to mimic variable fracture intensity. (**b**) Rose diagrams (plotted on top Cogollo depth map) showing fracture orientations in the Cogollo from borehole image logs and oriented cores. Dark blue lines show the interpreted orientation of maximum horizontal stress (SH_{max}). (**c**) Faults are represented by grid cells in the 3D model. The fault property shown here is *fault strike,* one parameter for the calculation of stress. (**d**) Normal stress values calculated at every fault cell. (**e**) Stress values are scaled to permeability range observed in the existing wells.

Hansen (2002) that resembles the methodology outlined by Akbar *et al*. (2003) and Wynn *et al*. (2005). The algorithms were set up directly in the geocellular modelling package, i.e. Petrel (Fig. 7), details of which are discussed in Pöppelreiter *et al*. (2005). The model requires the 3D representation of elastic rock properties, external stress field, and a relationship between stress and fracture permeability. These parameters are derived from regional tectonic knowledge, borehole image logs, density and sonic logs, pore pressure distribution, leak-off tests, laboratory tests, pressure tests and fault orientation (Zoback 2007). The vertical distribution of rock elastic properties was achieved by extending the sequence stratigraphic layering scheme with aspects of a mechanical stratigraphy. Tight layers were separated according to shaliness and thus their likelihood to be fractured (Fig. 7). Shaly units, earlier lumped with tight limestones, were separated out as they might have limited ascent of corrosive fluids, having neither matrix nor fracture permeability.

The output of the geomechanical model included normal and shear stress for every fault cell. The ratio of these stresses was used as semi-quantitative measure for the tendency of a fault to slip (Jaeger & Cook 1979). It was converted into fracture permeability (Bai & Elsworth 1994; Bai *et al*. 1999), thus representing the likelihood of corrosive fluids to circulate across (Fig. 7). The stress ratio was converted to width of leached zones (Fig. 8) by scaling it to the measured distance of elevated porosities near faults in existing wells. Thus, the width of leaching corridors was varied from 800 m to 2500 m in grainy facies, and a maximum of 200 m in muddy facies. Fault intersections, fault tip areas and relay zones (Fig. 6), particularly prone to migration of diagenetic fluids (Hickman *et al.* 2002, 2003) were screened using the Poly3D software (Stanford University) to predict likely areas with tensile and shear failure (Bourne *et al.* 2000, 2001). Selected fault intersections, fault tip areas and relay zones were separately modelled as 'leaching hot spots' about 5000 m in diameter. These were added to the leaching corridors described above. Subsequently, matrix porosity models for leaching corridors were created using porosity logs of wells with elevated porosities only. Different stochastic realizations were created.

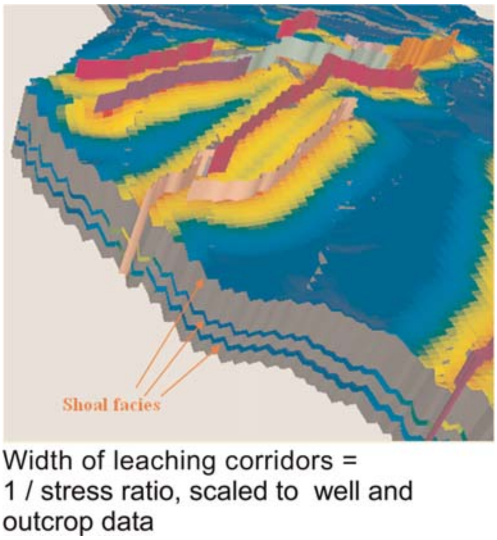

Fig. 8. Leaching corridors, i.e. areas with elevated porosities, are modelled along critically stressed, basement-rooted faults in grainy facies.

Charge-related diagenesis

Observations

Petrographic analysis showed that some of the secondary porosity (biomouldic, vuggy) in previously leached grainy facies was lost due to cementation, not because of facies change or lack of vuggy porosity. Cementation is commonly observed at structurally low areas of the field while structurally higher parts of the field commonly preserved some pore space in the thickest grainy beds along faults (Bartok *et al.* 1981). Those shallower areas might be less cemented because of early hydrocarbon charge as discussed for other areas by Marchand *et al*. (2002) and Wilkinson *et al*. (2006).

Modelling

Charge history and structural evolution at the greater Urdaneta West area were analysed to investigated the possibility of hydrocarbon fill having reduced cementation (Fig. 9). A basin model was used to reconstruct charge history. Results

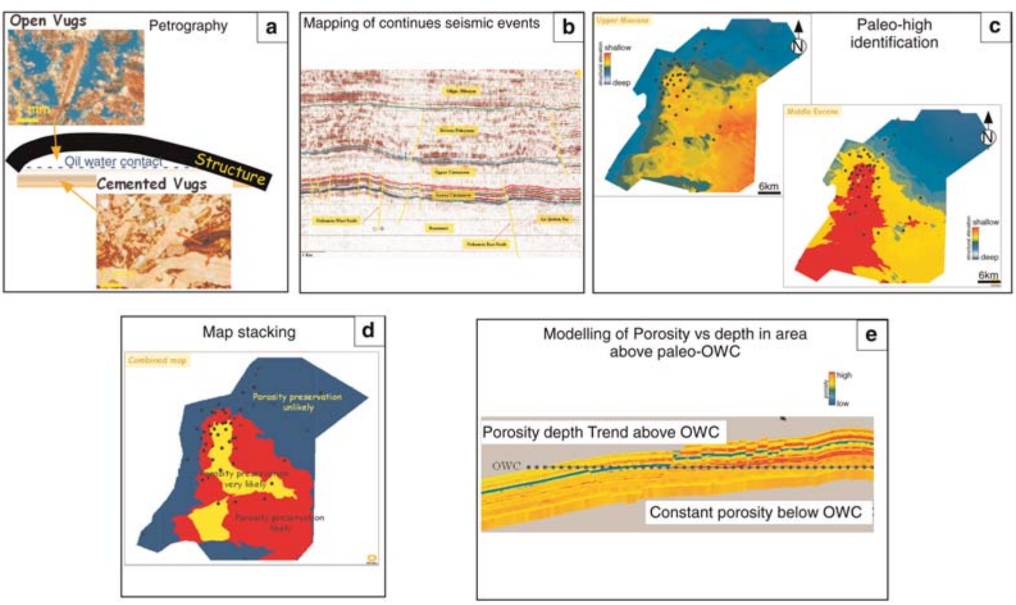

Fig. 9. Workflow used to model the effect of hydrocarbon charge on porosity distribution pattern. (**a**) Areas with lower porosities are commonly associated with cemented vugs as observed in cores and cuttings. (**b**) All possible continuous seismic events are mapped to investigate the structural evolution of top Cogollo. (**c**) Examples of the reconstructed top Cogollo structural configuration at Middle Eocene and Upper Miocene times (red = structurally shallow, blue = deep); (**d**) Two arbitrary oil columns (thick and thin) added to the top Cogollo map. Structurally high areas might have experienced less cementation due to early charge. Black dots indicate well locations. (**e**) Porosity modelling in palaeohigh area as function of height above palaeo-oil–water contact.

suggested first hydrocarbon charge occurred during Middle Eocene times (oral communication M. Nosiara 2003). Structural history was reconstructed using nine seismic depth maps of continuous, conformable seismic events. These horizons, ranging in age from Lower Cretaceous to Pliocene, were mapped across the field. The overburden layers were decompacted and the geometry of top Cogollo restored by flattening the individual seismic events. This study showed that an embryonic anticlinal structure started to develop at Urdaneta West from Middle Eocene times onward (Fig. 9). Subsequently, the nine individual depth maps were stacked. An area that remained structurally high through time emerged. An arbitrary oil column was added to the reconstructed top reservoir maps to estimate the extent of early charged structural highs (Fig. 9). Two scenarios, a thin and a thick oil column, were tested to estimate its impact on the extent of hydrocarbon-filled areas.

The region with the highest chance of accumulating hydrocarbons, and thus escaping cementation, was located in the southern part of the field. There is a good fit between this persistent structurally high area and the location of wells with better porosity. The outline of this structural high was superimposed on the 3D porosity model of fault-related leaching corridors to separate leached open from leached cemented regions.

Subsequently, porosity was modelled with a depth trend superimposed on the fault-leached porosity volume as described above. Porosity was modelled, in the palaeo-high areas, as a function of height above palaeo-oil–water contact (Fig. 9) to represent increasing cementation with decreasing oil saturation.

Fracturing

Observations

Production at Urdaneta West is dominated by matrix flow but well rates and pressure behaviour suggest the influence of fractures. Cores and image logs indicate fractures occur as unidirectional north-west–south-east striking joints and polydirectional fracture corridors next to faults. The degree of fracturing within individual layers seems to vary with mechanical properties, particularly shaliness (Li & Schmitt 1998).

Modelling

Layer-bound unidirectional joints are implemented as directional multipliers. Maps with specific factors for specific layers were used to increase matrix permeability to a level approximating productivity index and well behaviour. Fault-related fracture corridors (Trice 1999) are represented by specific grid cells. The width of fracture corridors was estimated from seismic semblance maps and image logs. These suggested widths of Jurassic fault zones of about 200 m, while Upper Carboniferous and Eocene faults are approximately 100 m wide. Fault zones were modelled in the geocellular model as discrete corridors represented by grid cells. Fault strike was assigned as a property to those cells (Fig. 7). The ratio of normal and shear stress, calculated from the geomechanical model was used to scale permeability to values similar to those derived from well analysis (Barton *et al.* 1995).

Results

The combination of several factors appears important for creating sufficiently porous zones at the Urdaneta West field. These included:

- early texture-controlled porosity-permeability network;
- conductive fracture network as conduits for corrosive fluids;
- regional aquifers and favourable fluid flow direction for corrosive fluids;
- hydrocarbon charge and trap formation; and
- layer-bound and fault-related fracture networks.

The integrated approach to analysis and modelling of reservoir property provided a tool to represent various property volumes that concur with the conceptual geological model and conform to the observed property patterns in existing wells. Thus, various geological scenarios were tested to estimate the impact on reservoir property distribution. Reservoir models were simulated and history-match was achieved adding confidence in the model results. The models highlighted the southern part of the field as a region with potentially better reservoir properties. These results were used for well planning in this geologically complex carbonate reservoir.

Conclusions

1. Geometries and pore systems of diagenetic zones are often complex and constitute a major uncertainty for field development.
2. Tectonic evolution might provide a template that controlled facies, diagenesis and reservoir property distribution. Its reconstruction may help to better understand and model complex diagenetic zones.
3. Burial diagenesis may be an important factor for porosity creation at the Urdaneta West field.

4. The extent of porous leaching zones was possibly controlled by the interplay of an early texture control porosity-permeability network, conductive structural conduits, and regional fluid flow via aquifers that transported corrosive fluids as well as hydrocarbon charge and trap evolution.

5. The use of trend maps and simple algorithms permitted the representation of a complex conceptual reservoir model using largely standard geocellular modelling tools. The workflow might assist in field development or exploration activities of diagenetically altered carbonate reservoirs in general.

We would like to acknowledge the contributions from our colleagues: A. Dombrowski, S. Engel, M. de Keijzer, X. Marquez, G. Sagasti, P. De Sousa and P. Wagner. The careful review by C. Cleneay improved the initial manuscript and is gratefully acknowledged. Specific comments by reviewers Mark Bentley and Richard Labourdette are very much appreciated, and helped to clarify aspects of the text. We wish to thank Shell Venezuela for their permission to publish this paper.

References

AKBAR, A. H., BROWN, T., DELGADO, R. *ET AL*. 2003. Watching rocks change–mechanical earth modelling. *Oilfield Review*, **2**, 22–39.

AZPIRITXAGA, I. 1991. *Carbonate depositional style controlled by siliciclastic influx and relative sea level changes, Lower Cretaceous Central Maracaibo Lake, Venezuela*. University of Austin, Master Thesis, 151pp.

BAI, M. & ELSWORTH, D. 1994. Modelling of subsidence and stress-dependent hydraulic conductivity for intact and fractured porous media. *Rock Mechanics and Rock Engineering*, **27**, 209–234.

BAI, M., FENG, F., ELSWORTH, D. & ROEGIERS, J.-C. 1999. Analysis of stress-dependent permeability in nonorthogonal flow and deformation fields. *Rock Mechanics and Rock Engineering*, **32**, 195–219.

BARTOK, P., REIJERS, T. J. A. & JUHASZ, I. 1981. Lower Cretaceous Cogollo Group, Maracaibo basin, Venezuela-sedimentology, diagenesis, and petrophysics. *AAPG Bulletin*, **65**, 1110–1134.

BARTON, C. A., ZOBACK, M. D. & MOOS, D. 1995. Fluid flow along potentially active faults in crystalline rock, *Geology*, **23**, 683–686.

BOREEN, T. D. & COLQUHOUN, K. 2003. The Ladyfern gas field–Canada is still hiding mammoths. *Abstracts AAPG Annual Meeting*, **12**, A17.

BOURNE, S. J., ITA, J. J., KAMPMAN-REINHARTZ, B. E., RIJKELS, L., STEPHENSON, B. J. & WILLEMSE, E. J. M. 2000. Integrated fractured reservoir modelling using geomechanics and flow simulation. *AAPG Bulletin*, 1395–1518.

BOURNE, S. J., RIJKELS, L., STEPHENSON, B.J. & WILLEMSE, E. J. M. 2001. Predictive modelling of naturally fractured reservoirs using geomechanics and flow simulation. *GeoArabia*, **6**, 27–42.

CASTILLO, M. V. & MANN, P. 2006. Cretaceous to Holocene structural and stratigraphic development in south Lake Maracaibo, Venezuela, inferred from well and three-dimensional seismic data. *AAPG Bulletin*, **90**, 529–565.

DAVIES, G. R. & SMITH, L. B., JR. 2006. Structurally controlled hydrothermal dolomite reservoir facies: An overview. *AAPG Bulletin*, **90**, 1641–1690.

EHRENBERG, S. N. & NADEAU, P. H. 2005. Sandstone vs. carbonate petroleum reservoirs: A global perspective on porosity-depth and porosity-permeability relationships. *AAPG Bulletin*, **89**, 435–445.

ESTEBAN, M. & TABERNER, C. 2003. Secondary porosity development during late burial in carbonate reservoirs as a result of mixing and/or cooling of brines. *Journal of Geochemical Exploration*, **79**, 355–359.

GALARRAGA, M., ENGEL, S. & HANSEN, B. 2005. *Detailed 3D seismic interpretation using HFI seismic data, fault throw and stress analysis for fault reactivation in the Cogollo group, Lower Cretaceous, Urdaneta West Field, Maracaibo Basin*. SPE n° 95060.

HANSEN, B. 2002. Geomechanics in 3D. Abstract of talk, Roxar user group meeting, Paris, Abstract volume.

HICKMAN, R. G., KENT, W. N., ODEGARD, M. E. & MARTIN, J. R. 2002. Where are the Trenton-Black River hydrothermal dolomite-hosted fields of the Illinois Basin? Abstract of talk, *AAPG 31st Annual Eastern Section Meeting*, *Conference Volume*, Champaign, Illinois.

HICKMAN, R. G., KENT, N. W., ODEGARD, M., HENSHAW, N. & MARTIN, J. 2003. *Hydrothermal Dolomite Reservoirs. A Play Whose Time Has Come*. Abstract of talk, AAPG Annual Convention, Salt Lake City, Abstract Volume.

HURLEY, N. F. & BUDROS, R. 1990. Albion-Scipio and Stoney Point fields–U.S.A. *In*: BEAUMONT, E. A. & FOSTER, N. H. (eds) *Stratigraphic Traps I: AAPG Treatise of Petroleum Geology Atlas of Oil and Gas Fields*, 1–37.

JAEGER, J. C. & COOK, N. G. W. 1979. *Fundamentals of Rock Mechanics*. (3rd edn) New York, Chapman & Hall, 28–30.

KNIPE, R. J. 1993. The influence of fault zone processes on diagenesis and fluid flow. *In*: HORBURY, A. D. & ROBINSON, A.G. (eds) *Diagenesis and Basin Development.* AAPG Studies in Geology, **36**, 135–151.

LI, Y. & SCHMITT, D. R. 1998. Drilling-induced core fractures and in situ stress. *Journal of Geophysical Research*, **103**, 5225–5239.

LOCKNER, D. A. & BEELER, N. M. 2002. Rock failure and earthquakes. *In*: LEE, W. K., KANAMORI, H., JENNINGS, P. & KISSLINGER, C. (eds) *International Handbook of Earthquake and Engineering Seismology*. San Diego, CA, Academic Press, **81A**, 505–537.

LOMANDO, A. J. 1999. Structural influence on facies trends of carbonate inner ramp systems, examples from the Kuwait–Saudi Arabian Coast of the Arabian Gulf and Northern Yucatan, Mexico. *GeoArabia*, **4**, 339–360.

LOPEZ-HORGUE, M. A., FERNANDEZ MENDIOLA, P. A., IRIARTE, E., SUDRIE, M., CALINE, B., GOMEZ, J.-P. & CORNEYLLIE, H. 2005. *Fault-related hydrothermal dolomite bodies in Early Cretaceous Platform*

Carbonates. Poster, 10th French Sedimentological Congress.

LUGO, J. M. 1991. *Cretaceous to Neogene tectonic control on sedimentation: Maracaibo basin, Venezuela*. PhD Thesis, University of Texas, Austin.

MARCHAND, M. E., SMALLEY, P. C., HASZELDINE, R. S. & FALLICK, A. E. 2002. Note on the importance of hydrocarbon fill for reservoir quality prediction in sandstones. *AAPG Bulletin*, **86**, 1561–1571.

PÖPPELREITER, M., BALZARINI, M. A., DE SOUSA, P. *ET AL*. 2005. Structural control on sweet spot distribution in a carbonate reservoir: Concepts and 3D Models (Cogollo Group, Lower Cretaceous, Venezuela). *AAPG Bulletin*, **89**, 1651–1676.

RENZ, O. 1981. Venezuela. *In*: REYMENT, R. A. & BENGSTON, P. (eds) *Aspects of Mid-Cretaceous Regional Geology*. Academic Press, New York, 197–220.

SCHOLLE, P. E. & HALLEY, R. B. 1985. Burial diagenesis: out of sight, out of mind! *In*: BEAUMONT, E. & FOSTER, N. H. (eds) *Reservoirs III*. Treatise of Petroleum Geology Reprint Series, **5**, 294–319.

TINKER, S. W., CALDWELL, D. H., COX, D. M., ZAHM, L. C. & BRINTON, L. 2004. Integrated reservoir characterization of a carbonate ramp reservoir, South Dagger Draw Field, New Mexico: seismic data are only part of the story. *In*: EBERLI, G., MASSAFERRO, J. L. & SARG, J. F. (eds) *Seismic Imaging of Carbonate Reservoirs and Systems*. AAPG Memoir, **81**, 91–105.

TRICE, R. 1999. Application of borehole image logs in constructing 3D static models of productive fractures in the Apulian Platform, Southern Apennines. *In*: LOVELL, M., WILLIAMSON, G. & HARVEY, P. (eds) *Borehole Imaging; Applications and Case Histories*. Geological Society, London, Special Publications, **159**, 155–176.

VAHRENKAMP, V. C., FRANSSEN, R. C. W. M., GRÖTSCH, J. & MUNOZ, P. J. 1993, Maracaibo Platform (Aptian-Albian), northwestern Venezuela. *In*: SIMO, J. A. T., SCOTT, R. W. & MASSE, J. P. (eds) *Cretaceous Carbonate Platforms*. AAPG Memoir, **25**, 25–33.

WILDE, A. R. & MUHLING, P. 2000. Comparison between the Lennard Shelf MVT Province of Western Australia and the Carlin Trend of Nevada: Implications for genesis and exploration. *In*: CLUER, J. K., PRICE, J. G., STRUHSACKER, E. M., HARDYMAN, R. F. & MORRIS, C. L. (eds) *Geology and Ore Deposits 2000: The Great Basin and Beyond*. Geological Society of Nevada Symposium Proceedings, 769–781.

WILKINSON, M., HASZELDINE, S. R. & FALLICK, A. E. 2006. Hydrocarbon filling and leakage history of a deep geopressured sandstone, Fulmar Formation, United Kingdom North Sea. *AAPG Bulletin*, **90**, 1945–1961.

WILSON, E. N. 1990. Dolomitisation front geometry, fluid flow patterns, and the origin of massive dolomites: The Triassic Latemar buildup, northern Italy. *American Journal of Science*, **290**, 741–796.

WYNN, T., BENTLEY, M., SMITH, S., SOUTHWOOD, D. & SPENCE, A. 2005. *In situ* stress properties in reservoir models. *In*: *The Future of Geological Modelling in Hydrocarbon Development*. Meeting abstract volume, **154**.

ZOBACK, M. D. 2007. *Reservoir geomechanics: earth stress and rock mechanics applied to exploration, production and wellbore stability*. Cambridge University Press.